Available online at www.sciencedirect.com
ScienceDirect
Solid State Communications 145 (2008) 56–60
solid state communications
www.elsevier.com/locate/ssc

Magneto-gyrotropic photogalvanic effects in GaN/AlGaN two-dimensional systems

W. Weber[a], S. Seidl[a], V.V. Bel'kov[a,b], L.E. Golub[b], S.N. Danilov[a], E.L. Ivchenko[b], W. Prettl[a], Z.D. Kvon[c], Hyun-Ick Cho[d], Jung-Hee Lee[d], S.D. Ganichev[a,*]

[a] *Terahertz Center, University of Regensburg, 93040 Regensburg, Germany*
[b] *A.F. Ioffe Physico-Technical Institute, Russian Academy of Sciences, 194021 St. Petersburg, Russia*
[c] *Institute of Semiconductor Physics, Russian Academy of Sciences, 630090 Novosibirsk, Russia*
[d] *Kyungpook National University, 1370 Sankyuk-Dong, Daegu 702-701, Republic of Korea*

Received 26 September 2007; accepted 26 September 2007 by S. Das Sarma
Available online 7 October 2007

Abstract

Magneto-gyrotropic photogalvanic and spin-galvanic effects are observed in (0001)-oriented GaN/AlGaN heterojunctions excited by terahertz radiation. We show that free-carrier absorption of linearly or circularly polarized terahertz radiation in low-dimensional structures causes an electric photocurrent in the presence of an in-plane magnetic field. Microscopic mechanisms of these photocurrents based on spin-related phenomena are discussed. Properties of the magneto-gyrotropic and spin-galvanic effects specific for hexagonal heterostructures are analyzed.

PACS: 73.21.Fg; 72.25.Fe; 78.67.De; 73.63.Hs

Keywords: A. Gallium nitride; A. Two-dimensional systems; D. Photogalvanic effects

1. Introduction

Gallium nitride is a promising semiconductor for spintronics since long spin relaxation times are detected in this material [1] and, if doped with manganese, it is expected to become ferromagnetic with a Curie temperature above room temperature [2]. Recently it has been shown that in GaN/AlGaN low-dimensional structures a substantial Rashba spin splitting in the electron band structure is present, potentially allowing spin manipulation by an external electric field [3]. The Rashba spin splitting due to structural inversion asymmetry, which is not expected in wide-band zinc-blende-based semiconductors, is caused in GaN wurtzite heterostructures by a large piezoelectric effect, which yields a strong built-in electric field at the GaN/AlGaN (0001) interface, and a strong polarization-induced doping effect [4,5]. Spin splitting in $\boldsymbol{k}$-space ($\boldsymbol{k}$ is the electron wave vector) may yield a variety of spin-dependent phenomena that can be observed in electronic transport and optical measurements. First indications of substantial spin splitting came from the observation of a circular photogalvanic effect in GaN/AlGaN heterojunctions [3]. Investigations of the circular photogalvanic effect were extended to GaN quantum wells as well as to GaN-based low dimensional structures under uniaxial stress confirming the Rashba-type of spin splitting [6, 7]. By weak-localization studies the magnitude of spin splitting has been obtained, showing that the splitting is comparable to that of GaAs-based heterostructures, being of the order of 0.3 meV at the Fermi wave vector [8–10]. On the other hand, measurements of Shubnikov–de Haas oscillations revealed a substantially larger spin splitting of about 1 meV [11].

Here we report on the observation of the magneto-gyrotropic photogalvanic effect (MPGE) [12–14] and the spin-galvanic effect [15–17] in GaN/AlGaN heterostructures. Both effects have been detected in (0001)-oriented structures in a wide range of temperatures from technologically important room temperature to liquid helium temperature. The microscopic

* Corresponding author. Tel.: +49 941 943 2050; fax: +49 941 943 1657.
E-mail address: sergey.ganichev@physik.uni-regensburg.de (S.D. Ganichev).

0038-1098/$ - see front matter © 2007 Elsevier Ltd. All rights reserved.
doi:10.1016/j.ssc.2007.09.035

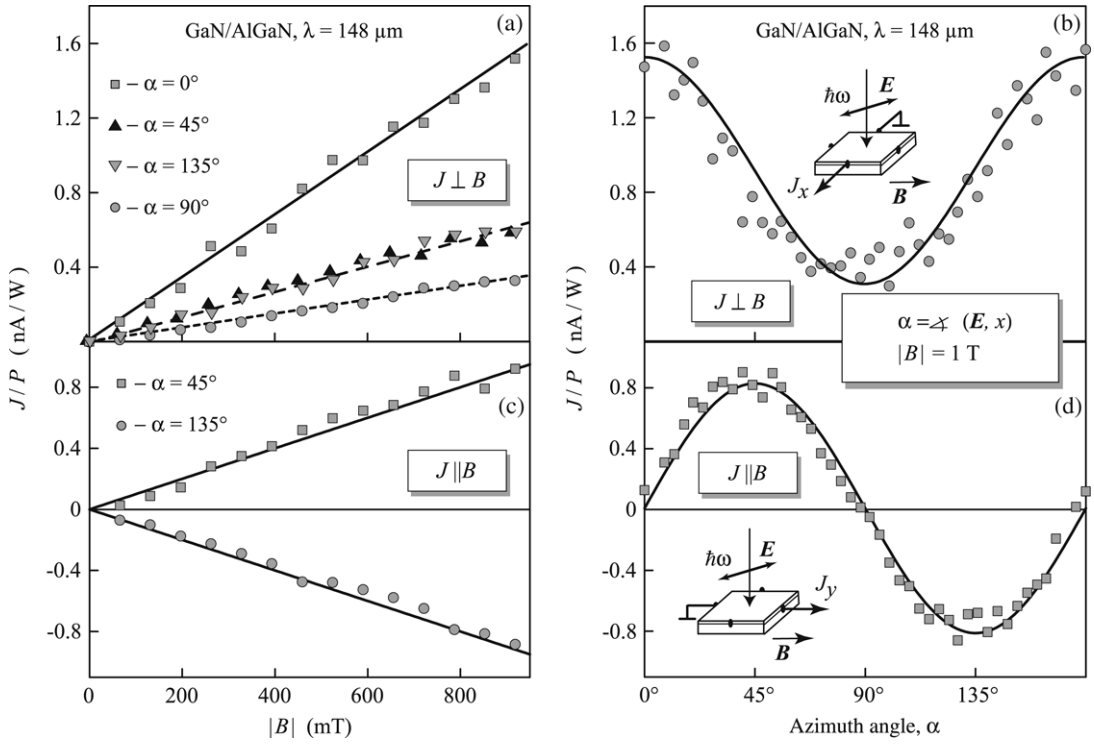

Fig. 1. Magnetic field and polarization dependences of the photocurrent $\boldsymbol{J} = [\boldsymbol{J}(\boldsymbol{B}) - \boldsymbol{J}(-\boldsymbol{B})]/2$ measured at room temperature in the transversal and longitudinal geometries. (a) and (c): magnetic field dependences of the magnetic-field-induced photocurrent at different azimuth angles α, (b) and (d): polarization dependences for transversal and longitudinal geometries, respectively. Photocurrent is excited by the normally incident linearly polarized radiation with power $P \approx 10$ kW. Full lines are the fits after Eqs. (4). The insets show the experimental geometries.

origin of the spin-galvanic effect is the inherent asymmetry of spin-flip scattering of electrons in systems with removed spin degeneracy of the electronic bands in $\boldsymbol{k}$-space [17]. The magneto-gyrotropic photogalvanic effect has so far been demonstrated in GaAs, InAs, and SiGe quantum wells where its microscopic origin is the zero-bias spin separation [13,14] which is caused by spin-dependent scattering of electrons due to a linear-in-$\boldsymbol{k}$ term in the scattering matrix elements. By the application of an external magnetic field, a pure spin current is converted into an electric current.

2. Samples and experimental methods

The experiments were carried out on $GaN/Al_{0.3}Ga_{0.7}N$ heterojunctions grown by MOCVD on a (0001)-oriented sapphire substrate with the electron mobility in the two-dimensional electron gas (2DEG) $\mu \approx 1200$ cm^2/V s at electron density $n_s \approx 10^{13}$ cm^{-2} at room temperature [3]. A high power THz molecular laser, optically pumped by a TEA–CO_2 laser [15], was used to deliver 100 ns pulses of linearly polarized radiation with a power of about 10 kW at wavelengths of $\lambda =$ 90.5 μm, 148 μm and 280 μm. The radiation causes indirect optical transitions within the lowest size-quantized subband. The samples were irradiated along the growth direction. Magnetic-field-induced photocurrents were investigated applying both linearly and circularly polarized radiation. In experiments the plane of polarization of linearly polarized light was rotated by applying a crystal quartz $\lambda/2$ plate. The circular polarization was obtained by means of a $\lambda/4$ plate. In this case the helicity of the incident light $P_{\rm circ} = \sin 2\varphi$ can be varied from -1 (left-handed circular, σ_-) to $+1$ (right-handed circular, σ_+) by changing the angle φ between the initial polarization plane and the optical axis of the $\lambda/4$ plate. An external magnetic field $\boldsymbol{B}$ up to 1 T was applied parallel to the heterojunction interface. To measure the photocurrent two pairs of ohmic contacts were centered along opposite sample edges (see insets in Fig. 1). The current $\boldsymbol{J}$, generated by the light in the unbiased devices, was measured via the voltage drop across a 50 Ω load resistor in a closed-circuit configuration. The voltage was recorded with a storage oscilloscope.

3. Experimental results

Irradiating a (0001) GaN/AlGaN heterojunction by linearly polarized light at normal incidence, as sketched in insets of Fig. 1, we observe a photocurrent signal in both perpendicular (transversal geometry, Fig. 1(a), (b)) and parallel (longitudinal geometry, Fig. 1(c), (d)) to the magnetic field $\boldsymbol{B}$ directions. The width of the current pulses is about 100 ns, which corresponds to the terahertz laser pulse duration. The photocurrent is proportional to the magnetic field strength and its sign depends on the magnetic field direction. Fig. 1(a) and (c) show the magnetic field dependence of the photocurrent for both geometries and for various orientation of the polarization plane of linearly polarized radiation in respect to the magnetic field direction. In these figures

$$\boldsymbol{J} = [\boldsymbol{J}(\boldsymbol{B}) - \boldsymbol{J}(-\boldsymbol{B})]/2$$

is plotted in order to extract the magnetic-field-induced photocurrent from the total current which contains a

small magnetic-field-independent contribution caused by the magnetic-field-independent linear photogalvanic effect [15,16]. Fig. 1(b) and (d) demonstrate that the photocurrent exhibits an essentially different polarization dependence for longitudinal and transversal geometries. While upon the variation of the azimuth angle α the sign of the transversal photocurrent remains unchanged, the longitudinal current changes its direction by switching α from $+45°$ to $-45°$ at constant magnetic field. We find that the polarization dependence of the current $\boldsymbol{J}$ in transversal geometry $\boldsymbol{J} \perp \boldsymbol{B}$ is well fitted by $J_\perp = J_1 \cos 2\alpha + J_2$, and for the longitudinal geometry $\boldsymbol{J} \parallel \boldsymbol{B}$ by $J_\parallel = J_3 \sin 2\alpha$ and $J_1 \approx J_3$. Below we demonstrate that exactly these dependences come out from the phenomenological theory. Using two fixed polarization states in the transversal geometry, $\alpha = 0°$ and $\alpha = 90°$, allows us to extract J_1 and J_2. Adding and subtracting the currents of both polarizations the polarization-dependent contribution J_1 and polarization-independent contribution J_2 can be obtained by

$$J_1 = \frac{J_\perp(\alpha = 0°) - J_\perp(\alpha = 90°)}{2}, \qquad (1)$$
$$J_2 = \frac{J_\perp(\alpha = 0°) + J_\perp(\alpha = 90°)}{2}.$$

Fig. 2 shows the temperature dependences of J_1 and J_2 together with the electron density and mobility. It is seen that the qualitative behaviour of both contributions is similar: at low temperatures they are almost independent of temperature, but at high temperatures (for J_1 at $T > 50$ K and for J_2 at $T > 100$ K) the current strength decreases with temperature increasing.

In addition to the magnetic-field-induced photocurrent excited by linearly polarized radiation we also observed a signal in response to circularly polarized light. While in the transversal geometry the signal is insensitive to the switching of the radiation helicity from σ_+ to σ_-, in the longitudinal geometry this operation results in the reversal of the current direction. Fig. 3 shows the dependence of the photocurrent on the angle φ. These data can be well fitted by $J_\parallel = J_4 \sin 4\varphi + J_5 \sin 2\varphi$. The fit, also shown in Fig. 3, yields the ratio $J_4/J_5 \approx 5$ at room temperature.

4. Discussion

Polarization and magnetic field dependences as well as the difference in the photocurrent behaviour for longitudinal and transversal geometries can be obtained in the framework of the phenomenological theory of the MPGE, which yields [12]

$$j_\alpha = I \sum_{\beta\gamma\delta} \phi_{\alpha\beta\gamma\delta} B_\beta \frac{e_\gamma e_\delta^* + e_\delta e_\gamma^*}{2} + I \sum_{\beta\gamma} \mu_{\alpha\beta\gamma} B_\beta \hat{e}_\gamma P_{\mathrm{circ}}. \qquad (2)$$

Here $\boldsymbol{j}$ is the photocurrent density proportional to $\boldsymbol{J}$, I the light intensity inside the heterostructure, $\hat{\boldsymbol{\phi}}$ the fourth-rank tensor symmetric in the last two indices, $\hat{\boldsymbol{\mu}}$ the third-rank tensor, $\boldsymbol{e}$ the light polarization vector, and $\hat{\boldsymbol{e}}$ a unit vector in the light

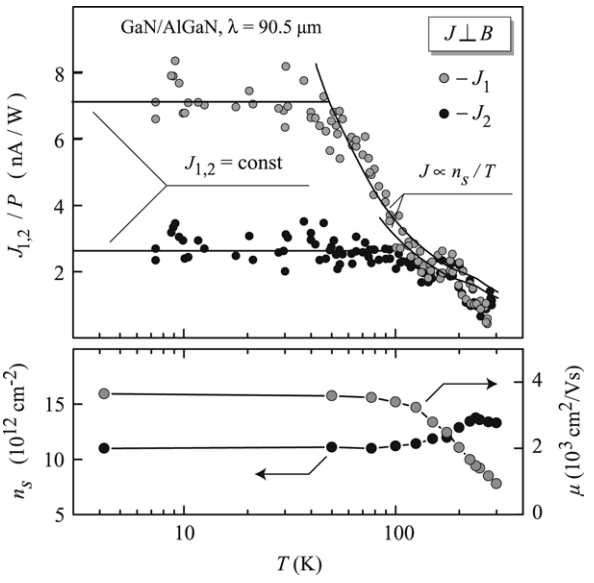

Fig. 2. Upper panel: Temperature dependences of the transversal magnetic-field-induced photocurrent. Data are obtained for $|B_y| = 0.6$ T and an excitation at $P \approx 10$ kW. Photocurrents $J_1(T)$ and $J_2(T)$ are obtained by subtracting and adding the currents for the two polarizations: $J_\perp(\alpha = 0°)$ and $J_\perp(\alpha = 90°)$ (see Eq. (1)). Full lines are fits of $J_1(T)$ and $J_2(T)$ to $A \cdot n_s(T)/k_B T$, with a scaling parameters A, and to a constant, respectively. The lower panel shows the temperature dependences of the carrier density n_s and the electron mobility.

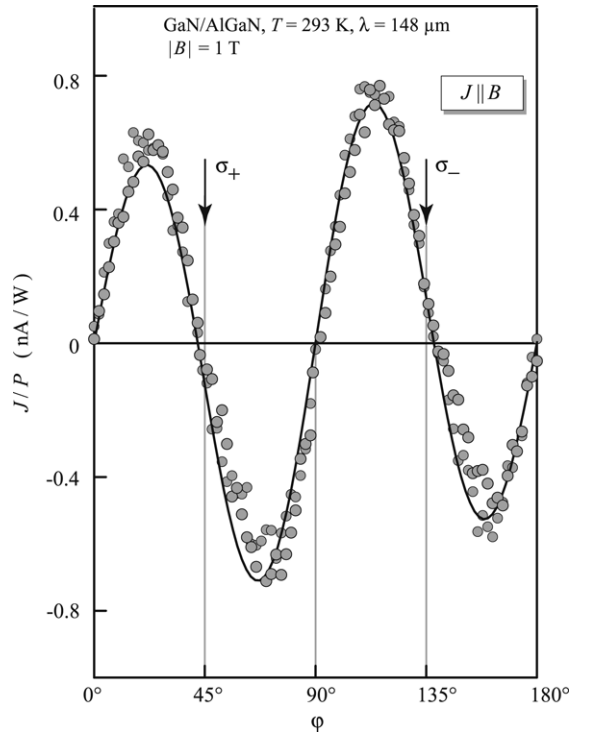

Fig. 3. Magnetic-field-induced photocurrent $\boldsymbol{J}$ as a function of the phase angle φ defining the radiation helicity. The photocurrent signal is measured at room temperature in the longitudinal geometry $\boldsymbol{J} \parallel \boldsymbol{B}$ under normal incidence of the radiation with $P \approx 10$ kW. The full line is the fit after the second equation of Eqs. (5).

propagation direction. While the second term in the right-hand side of the Eq. (2) requires circularly polarized radiation the first term may be non-zero for any, even unpolarized, radiation.

The point-group symmetry of (0001)-grown GaN-based low-dimensional structures is C_{3v}. The symmetry analysis for the C_{3v} point group shows that Eq. (2) for normal light incidence reduces to

$$\begin{aligned} j_x &= I S_1 B_y - I S_2 B_x (e_x e_y^* + e_y e_x^*) \\ &\quad + I S_2 B_y (|e_x|^2 - |e_y|^2) + I \mu B_x P_{\mathrm{circ}}, \\ j_y &= -I S_1 B_x + I S_2 B_y (e_x e_y^* + e_y e_x^*) \\ &\quad + I S_2 B_x (|e_x|^2 - |e_y|^2) + I \mu B_y P_{\mathrm{circ}}. \end{aligned} \tag{3}$$

Here three linearly independent constants are introduced as follows: $S_{1,2} = (\phi_{xyxx} \pm \phi_{xyyy})/2$, and $\mu = \mu_{xxz}$. Note that Eqs. (3) are also valid for the C_{6v} symmetry of bulk hexagonal GaN and even for uniaxial systems of the $C_{\infty v}$ symmetry. The form of these equations is invariant under a transfer from a given coordinate frame (x, y) to another one obtained by the rotation around the z axis by any azimuth angle. The fact that the photocurrents in both directions are described by only three coefficients (S_1, S_2, and μ) is in contrast to the MPGE in systems of the C_{2v} symmetry [12], where in the similar equations all coefficients in the eight terms in the right-hand sides of Eqs. (3) are linearly independent.

Eqs. (3) can be directly applied to describe polarization dependences in longitudinal and transversal geometries. For the geometry used in our experiment where the counterclockwise azimuth angle α between the x axis and the unit vector of linear polarization is varied, the polarization-dependent factors in Eqs. (3) can be written as $|e_x|^2 - |e_y|^2 = \cos 2\alpha$, $e_x e_y^* + e_y e_x^* = \sin 2\alpha$ and $P_{\mathrm{circ}} = 0$. According to Eqs. (3) for a fixed direction of the magnetic field, say $B \parallel y$, the photocurrent in response to the linearly polarized radiation is given by

$$\begin{aligned} j_x &= I B_y (S_1 + S_2 \cos 2\alpha), \\ j_y &= I B_y S_2 \sin 2\alpha. \end{aligned} \tag{4}$$

Fits of experimental data to these equations are shown in Fig. 1(b) and (d), demonstrating a good agreement with the theory. We emphasize (i) the presence of a substantial contribution of the polarization-independent first term on the right-hand side of the Eq. (4) to the current j_x, and (ii) the equal amplitudes of the α-dependent contributions for both transversal and longitudinal geometries.

For elliptically polarized light obtained in experiments by varying the angle φ between the initial polarization plane and the optical axis of the $\lambda/4$ plate the polarization-dependent terms are described by $|e_x|^2 - |e_y|^2 = (1 + \cos 4\varphi)/2$, $e_x e_y^* + e_y e_x^* = \sin 4\varphi/2$ and $P_{\mathrm{circ}} = \sin 2\varphi$. Thus for a magnetic field applied along y, Eqs. (3) take the form

$$\begin{aligned} j_x &= I B_y \left(S_1 + S_2 \frac{1 + \cos 4\varphi}{2} \right), \\ j_y &= I B_y \left(S_2 \frac{\sin 4\varphi}{2} + \mu \sin 2\varphi \right). \end{aligned} \tag{5}$$

These equations show that the contribution to the magnetic-field-induced photocurrent is expected from the last term in the right-hand side of the second equation described by the coefficient μ. The fit of our data by Eqs. (5) presented in Fig. 3 demonstrates a good agreement between the experiment and the theory. Furthermore, as an essential result, it follows from Fig. 3 that the current proportional to the radiation helicity and described by the coefficient μ is clearly measurable. At excitation by circularly polarized radiation the term containing S_2 vanishes and the current which remains is that due to the term with μ only. It changes its sign by switching from σ_+ to σ_- as observed in experiment.

Microscopically the magnetic-field-induced photocurrent proportional to the radiation helicity P_{circ} is caused by the spin-galvanic effect previously reported for GaAs- and InAs-based two-dimensional structures [17]. The effect is due to the optical orientation of carriers followed by the Larmor precession of the oriented electronic spins in the magnetic field and asymmetric spin relaxation processes (for details see Refs. [15–17]). Though, in general, the spin-galvanic current does not require the application of a magnetic field, it may be considered as a magnetophotogalvanic effect under the above experimental conditions. The photocurrent described by the coefficient S_2, as well as by S_1, is caused by the magneto-gyrotropic photogalvanic effect [12–14]. The microscopic mechanism of the MPGE in low-dimensional structures has been developed most recently to describe this effect in GaAs-, InAs-, and SiGe-based structures [13,14]. It has been shown that free carrier absorption of THz radiation results in a pure spin current and corresponding spin separation achieved by spin-dependent scattering of electrons in gyrotropic media. The pure spin current in these experiments was converted into an electric current by application of a magnetic field which polarizes spins due to the Zeeman effect. The key experiment supporting this microscopic mechanism is investigation of the temperature dependence of the photocurrent: the photocurrent due to zero-bias spin separation should be constant at low temperatures and should behave as the ratio $n_s(T)/k_B T$ at high temperatures [13,14]. Fig. 2 shows that the temperature dependences of J_1 and J_2 contributions indeed can be well fitted by constant factors in the low temperature range and vary as $n_s(T)/k_B T$ at high temperatures. Furthermore in the range 50–100 K where the mobility is almost constant the magnitude of J_1 changes rapidly, showing that J and μ are not correlated. The temperature behaviour of the photocurrent demonstrates the applicability of the discussed above model to the MPGE photocurrent observed in GaN/AlGaN heterojunctions. We note, however, that the influence of the magnetic field on electron scattering [18,19] may also result in a photocurrent yielding an additional contribution to the MPGE [20]. Since the microscopic origin of both contributions is different, the relative role of them can be clarified by additional experiments, e.g. by the variation of g-factor in Mn-doped nitride low-dimensional structures.

5. Conclusion

In summary, we demonstrated that the presence of a substantial gyrotropy in GaN/AlGaN heterostructures gives a

root to the spin-galvanic effect and the magneto-gyrotropic photogalvanic effect. We note that in our GaN heterojunctions the MPGE and spin-galvanic current contributions have the same order of magnitude. Both effects have been proved to be an effective tool for investigation of nonequilibrium processes, in-plane symmetry and inversion asymmetry of heterostructures, electron momentum and spin relaxation etc., and, therefore, may be used for investigation of this novel material attractive for spintronics.

Acknowledgments

The financial support of the DFG, RFBR and RSSF is gratefully acknowledged. E.L.I. thanks DFG for the Merkator professorship.

References

[1] B. Beschoten, E. Johnston-Halperin, D.K. Young, et al., Phys. Rev. B 63 (2001) 121202.
[2] T. Dietl, H. Ohno, F. Matsukura, J. Cibert, D. Ferrand, Science 287 (2000) 1019.
[3] W. Weber, S.D. Ganichev, S.N. Danilov, et al., Appl. Phys. Lett. 87 (2005) 262106.
[4] R. Cingolani, A. Botchkarev, H. Tang, et al., Phys. Rev. B 61 (2000) 2711.
[5] V.I. Litvinov, Phys. Rev. B 68 (2003) 155314.
[6] K.S. Cho, Y.F. Chen, Y.Q. Tang, et al., Appl. Phys. Lett. 90 (2007) 041909.
[7] X.W. He, B. Shen, Y.Q. Tang, et al., Appl. Phys. Lett. 91 (2007) 071912.
[8] S. Schmult, M.J. Manfra, A. Punnoose, et al., Phys. Rev. B 74 (2006) 033302.
[9] N. Thillosen, S. Cabañas, N. Kaluza, et al., Appl. Phys. Lett. 88 (2006) 022111.
[10] C. Kurdak, N. Biyikli, Ü. Özgür, H. Morkoc, V.I. Litvinov, Phys. Rev. B 74 (2006) 113308.
[11] N. Tang, B. Shen, M.J. Wang, et al., Appl. Phys. Lett. 88 (2006) 172112.
[12] V.V. Bel'kov, S.D. Ganichev, E.L. Ivchenko, et al., J. Phys. C: Condens. Matter 17 (2005) 3405.
[13] S.D. Ganichev, V.V. Bel'kov, S.A. Tarasenko, et al., Nature Phys. 2 (2006) 609.
[14] S.D. Ganichev, S.N. Danilov, V.V. Bel'kov, et al., Phys. Rev. B 75 (2007) 155317.
[15] S.D. Ganichev, W. Prettl, Intense Terahertz Excitation of Semiconductors, Oxford University Press, Oxford, 2006.
[16] E.L. Ivchenko, Optical Spectroscopy of Semiconductor Nanostructures, Alpha Science Int., Harrow, 2005.
[17] S.D. Ganichev, E.L. Ivchenko, V.V. Belkov, et al., Nature 417 (2002) 153.
[18] O.V. Kibis, Phys. Lett. A 244 (1998) 432.
[19] A.G. Pogosov, M.V. Budantsev, O.V. Kibis, et al., Phys. Rev. B 61 (2000) 15603.
[20] H. Diehl, V.A. Shalygin, S.N. Danilov, et al., J. Phys.: Condens. Matter 19 (2007) 436232.